

Measuring the strong electrostatic and magnetic fields with proton radiography for ultra-high intensity laser channeling on fast ignitiona)

Y. Uematsu, S. Ivancic, T. Iwawaki, H. Habara, A. L. Lei, W. Theobald, and K. A. Tanaka

Citation: [Review of Scientific Instruments](#) **85**, 11E612 (2014); doi: 10.1063/1.4890575

View online: <http://dx.doi.org/10.1063/1.4890575>

View Table of Contents: <http://scitation.aip.org/content/aip/journal/rsi/85/11?ver=pdfcov>

Published by the [AIP Publishing](#)

Articles you may be interested in

[Soft x-ray backlighting of cryogenic implosions using a narrowband crystal imaging system \(invited\)a\)](#)

Rev. Sci. Instrum. **85**, 11E501 (2014); 10.1063/1.4890215

[Hydrodynamic instability growth and mix experiments at the National Ignition Facilitya\)](#)

Phys. Plasmas **21**, 056301 (2014); 10.1063/1.4872026

[Study of ultraintense laser propagation in overdense plasmas for fast ignitiona\)](#)

Phys. Plasmas **16**, 056307 (2009); 10.1063/1.3101912

[Proof of principle experiments that demonstrate utility of cocktail hohlraums for indirect drive ignitiona\)](#)

Phys. Plasmas **14**, 056311 (2007); 10.1063/1.2712426

[Review of progress in Fast Ignitiona\)](#)

Phys. Plasmas **12**, 057305 (2005); 10.1063/1.1871246



AIP | Journal of
Applied Physics

Journal of Applied Physics is pleased to
announce **André Anders** as its new Editor-in-Chief

Measuring the strong electrostatic and magnetic fields with proton radiography for ultra-high intensity laser channeling on fast ignition^{a)}

Y. Uematsu,¹ S. Ivancic,² T. Iwawaki,¹ H. Habara,^{1,b)} A. L. Lei,³ W. Theobald,² and K. A. Tanaka¹

¹Graduate School of Engineering, Osaka University, Osaka 565-0871, Japan

²Laboratory for Laser Energetics, 250 East River Road, Rochester, New York 14623-1299, USA

³Shanghai Institute of Laser Plasma, 201800 Shanghai, China

(Presented 3 June 2014; received 1 June 2014; accepted 8 July 2014; published online 11 August 2014)

In order to investigate the intense laser propagation and channel formation in dense plasma, we conducted an experiment with proton deflectometry on the OMEGA EP Laser facility. The proton image was analyzed by tracing the trajectory of mono-energetic protons, which provides understanding the electric and magnetic fields that were generated around the channel. The estimated field strengths ($E \sim 10^{11}$ V/m and $B \sim 10^8$ G) agree with the predictions from 2D-Particle-in-cell (PIC) simulations, indicating the feasibility of the proton deflectometry technique for over-critical density plasma.

© 2014 AIP Publishing LLC. [<http://dx.doi.org/10.1063/1.4890575>]

I. INTRODUCTION

In the fast ignition (FI) of inertial confinement fusion,¹ an ultra-high intensity laser heats the dense plasma core to trigger the thermonuclear fusion reactions. In this scheme, it is crucially important to investigate the laser propagation into the imploded plasma. When the laser irradiates the coronal region, the laser creates a low-density plasma channel by ponderomotive evacuation of the bulk electrons inside the laser beam with the formation of strong electrostatic field at the edge of the channel. A strong magnetic field is also created by forward electron acceleration. Proton deflectometry is one of the fascinating techniques to observe the plasma channel through the measurement of these electromagnetic fields.² Especially, investigation of the laser propagation in an over-critical density plasma is significantly important for the direct irradiation scheme of a single intense laser beam, “Super-penetration,”³ which stands on the relativistic effects such as relativistic self-focusing and relativistic transparency, followed by plasma channel formation by hole-boring.

For this purpose, we conducted a plasma channeling experiment at OMEGA EP laser facility in University of Rochester. A proton beam from a point source passed through the channel perpendicular to its axis and was deflected according to the electric and magnetic fields embedded inside the channel. The transmitted proton beam deposited its energy on Radio Chromic Film (RCF) and the detected image was analyzed by calculating the trajectory of mono-energetic protons in order to estimate the E and B field distributions. The analysis implies the formation of a single straight channel up to a density between n_c and $n_c/2$, where n_c stands for the critical density, which was also observed in a separate optical

measurement.⁴ This result indicates the feasibility of the application of time-resolved proton radiography to plasma densities higher than the critical density.

II. SETUP

A. Experiment

The experimental setup is shown in Fig. 1(a). Two long UV laser pulses ($\lambda = 351$ nm) irradiate a thin plastic foil ($3 \text{ mm} \times 3 \text{ mm}$, $120 \mu\text{m}$ thickness) to create a long scale-length plasma. The UV laser energy was in totally 1 kJ. The pulse duration was 1 ns and the beams were smoothed by distributed phase plates⁵ with a focal spot size of $800 \mu\text{m}$ diameter. An ultra intense laser beam (BL) was then injected into the plasma to create a plasma channel inside it. The laser energy was 1250 J with 10 ps pulse duration operated at 1ω ($\lambda = 1053$ nm). In order to produce a point-source proton beam, another 1ω short pulse laser (SL) is irradiated on a $20 \mu\text{m}$ thin copper foil with 830 J energy and 10 ps pulse duration. The created proton beam had an energy range of up to 50 MeV and was detected with a stack of 18 RCFs (HD810) at the opposite side of the plasma. The magnification of the image was set to be 10.

The irradiation timing among beams is illustrated in Fig. 1(b). The BL beam was injected into the plasma 500 ps after the UV beams were terminated. By taking into account the proton beam arrival at the interaction point, the SL beam was fired at 100 ps before the BL beam, resulting in a temporal observation windows from -24 ps to 82 ps relative to the BL injection timing. Fig. 1(c) shows the calculated electron density profile prior to BL injection from a 2D radiation hydrodynamic simulation with the code DRACO.⁶ The BL laser was focused to the position $750 \mu\text{m}$ in front of the initial target surface, corresponding to $n_c/4$ for maximizing the channel length.³ The density scale length was $250 \mu\text{m}$ at $n_c/4$ in this experiment.

^{a)}Contributed paper, published as part of the Proceedings of the 20th Topical Conference on High-Temperature Plasma Diagnostics, Atlanta, Georgia, USA, June 2014.

^{b)}habara@eei.eng.osaka-u.ac.jp.

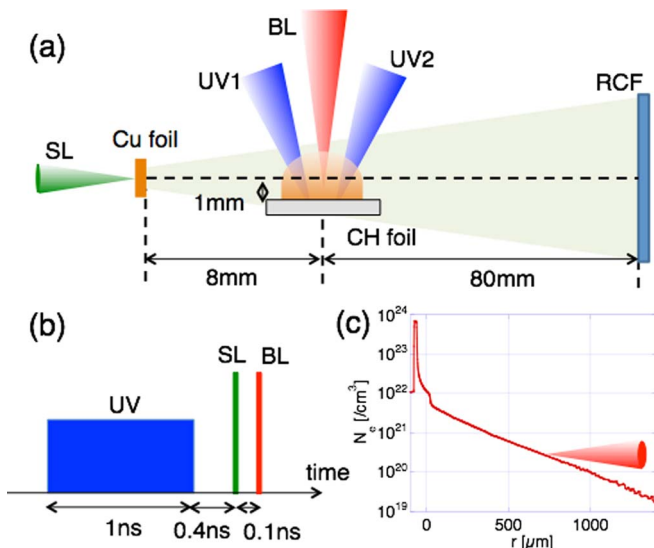


FIG. 1. (a) Experimental setup. UV1 and 2: 3ω laser for plasma creation, BL: 1ω laser for plasma channel formation, and SL: 1ω laser for point source proton beam. (b) Irradiation timing among all laser beams. (c) Plasma density profile at the channeling beam irradiation calculated by DRACO code.⁵

B. Track calculation

In order to reproduce the proton deflectometry image, we calculated proton trajectories from the source position via the Monte Carlo method. In this calculation, initial energy and momentum of each proton were allocated randomly according to the given momentum distribution. Once a proton arrives at the plasma region, the position and the direction of the proton are updated according to the electromagnetic force ($F = q(E + v \times B)$) until the proton leaves the plasma region. Finally, the dose on the RCF film, calculated from the proton energy and incident angle to the RCF, is accumulated for all protons.

III. EXPANDED PLASMA COLONA

Different from the gas jet target, the free-expanding plasma created in front of the planar target usually involves an electric fields at its boundary by plasma pressure⁷ as well as magnetic field due to non-collinear density and temperature gradient ($\nabla n_e \times \nabla T_e$).⁸ These fields may affect the proton trajectory before and after the propagation through the channel region. However, this magnetic field is a poloidal field around the target normal direction, so that the side-on geometry of proton deflectometry is insensitive to the magnetic field due to the counteracting effect on the proton motion going in and out of the plasma.⁹ Therefore, only the E-field should be taken into account for this analysis.

Figure 2(a) shows the observed image taken with 22 MeV protons corresponding to 24 ps prior to the peak of the 10-ps channeling beam. The laser propagated from the right to the left in this figure. Although the high-energy UV beams were already terminated, the target still exists at the initial position without significant deformation. The pileup of protons at the edge of the plasma is clearly visible. The size of plasma is slightly larger than the UV spot size ($800 \mu\text{m}$) due to the

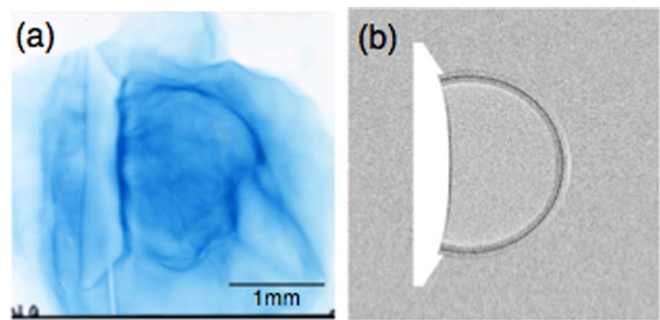


FIG. 2. (a) Side-on proton image of the long-scale-length plasma taken with RCF before the arrival of the channeling pulse. (b) Reconstructed image.

spherical expansion. Figure 2(b) shows the reproduced proton image using monochromatic 22 MeV protons. The width of the edge strongly depends on the electric field strength. As the result of comparison to the experimental data, we conclude that the strength of radial electric field at the edge ranges from 2×10^9 to 5×10^9 V/m, which agrees well with the simulation result in Ref. 6 where similar laser energy was used for plasma creation. We also applied the magnetic field in the calculation with the strength used in Ref. 7, but the edge structure is significantly insensitive to the magnetic field strength as expected. According to Ref. 6, the radial electric fields exist inside the plasma with 1/5–1/10 of the edge electric field strength. This inner field acts as a negative lens for the proton beam giving further expansion of the image around the center. We checked this further expansion of the image, resulting in less than 27% and 15% for 9 MeV and 22 MeV protons, respectively. This additional expansion is not large, but was taken into account in the analysis of the channel image.

IV. PLASMA CHANNEL

Figure 3(a) shows a 9.4 MeV proton image (calibrated proton number distribution¹⁰) detected 82 ps after the BL laser irradiated the expanding plasma. The thick dashed contour on the left side represents the initial target position. In addition, the half circle dotted curve at the right edge indicates the position of the plasma boundary. Although there are many fine structures in the image, we analyzed the relatively large structure indicated by horizontal dotted lines. In the center part of this structure, there is a slightly lighter region surrounded by upper and lower darker bands, and these sizes decrease along the laser propagation direction (from the right to the left in this image).

Assuming that this structure indicates the plasma channel, we conducted proton tracking calculations in order to reproduce this image as shown in Fig. 3(b). In the calculation, we incorporated electric and magnetic field structures predicted by a 2D PIC calculation. Figs. 3(b) and 3(c) show snapshots of the radial electrostatic field (E_y) and azimuthal magnetic field (B_z) when a 1ω laser pulse with an intensity of 10^{19} W/cm² propagated in a long homogenous plasma column with a density of n_c . The electric fields were created at the channel wall. One can see the reversal of the sign of the field direction at the wall. This structure was observed at a later time of the simulation ($>$ several 100 fs) and was

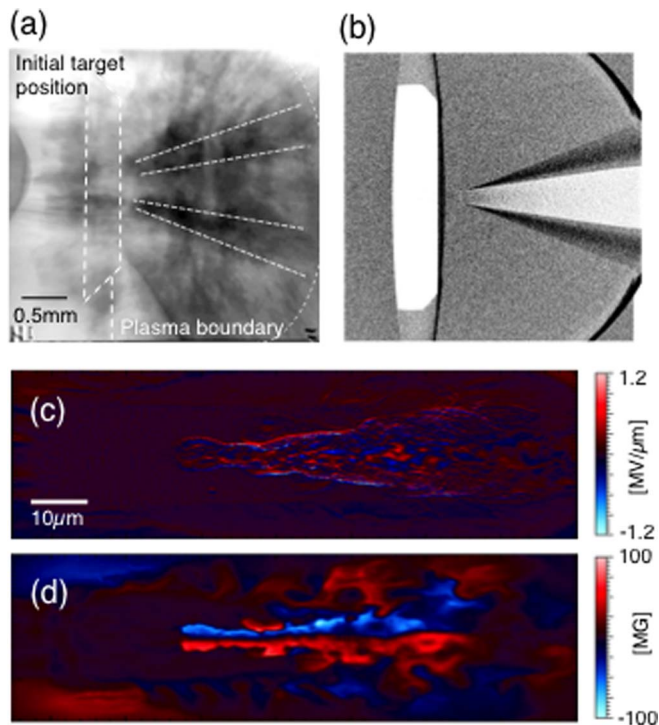


FIG. 3. (a) Experimental results taken with 9.4 MeV protons corresponding to 82 ps after the BL beam injection. (b) Calculation results of the proton image. (c) Electric and (d) magnetic field distributions calculated by a 2D-PIC calculation of a 1×10^{19} W/cm² laser light propagating in a critical density plasma.

formed by localization of ions moving with the electron sheath field created due to space charge separation in the electron-evacuated channel. The thickness of E-field layer strongly depends on the simulation conditions, so that we also changed the thickness in the calculation. On the other hand, the magnetic field is created by the forward fast electron current and is enhanced by the backward return current. The strength of the magnetic field is larger than 100 MG, which is also comparable to the laser B-field.

In the track calculation, proton energy is fixed to be 9.4 MeV same as the experiment. The time steps inside and outside of the channel are 1 and 10 fs, respectively. From the separate measurement using an UV optical probe⁴ in this shot, the plasma channel seems to be generated up to 0.5 mm from the initial target surface. Also we assume F/2.0 cone angle for channel shape from the f-number of the parabolic mirror that focused the BL beam. The well-reproduced calculation results are shown in Fig. 3(b). When the protons come close to the plasma channel, the proton motion is bent by the Lorentz force, which can form a central pale structure and outer dark regions as shown both in the experiment and calculation. In the calculation, the stronger electric field reduces the vertical length of the dark region because of confinement of the proton beam due to the inner electric field. On the other hand, different from the calculation of the coronal plasma, strong azimuthal magnetic field inside the channel can affect the proton trajectory. The magnetic field helps to expand the dark regions not only in the radial regions but also in the horizontal direction toward the laser entrance. This

is caused by the assumption that the field strength is in proportion to the channel diameter. The magnetic field bends the proton to the laser (left) direction when the protons go out of the plasma with preserving the larger radial momentum given by the weaker inner electric field. As a result of the calculation, the maximum electric field is 0.1 (± 0.05) MV/μm and the magnetic field is 55 (± 5) MG from the comparison of the widths of the white and dark regions (the error of the width corresponds to the error of fields strengths of $\sim 10\%$ in average), which are 3% and 17% of laser fields, respectively.

V. SUMMARY

In order to investigate the intense laser beam propagation in dense plasma, we conducted an experiment with proton deflectometry at the OMEGA EP Laser Facility. The proton image was analyzed by tracing the trajectory of monoenergetic protons, which allows one to estimate the E and B field strengths in the plasma. The observed proton image can be reproduced in calculations assuming the field distributions extracted by 2D-PIC simulations. At an early time before the channeling pulse arrived, a plasma channel was not observed but the boundary of blow off plasma clearly appeared as in experiments reported by other groups. At a later timing, shortly after the channeling pulse arrival, a large structure in the detected image indicates a plasma channel. Comparing both calculation and experiment, the estimated field strengths ($E \sim 10^{11}$ V/m and $B \sim 10^9$ G) embedded in this structure are comparable to the simulation results. Our study makes a progress to understanding of the physics of the propagation of an intense laser pulse in imploded plasma, and helps for estimating the required laser conditions for direct heating scheme fast ignition.

ACKNOWLEDGMENTS

This work was fully supported by Japan/U.S. Cooperation in Fusion Research and Development in 2012 and 2013. Part of this work was performed under “ASHULA” Asian Core Program and Grants-in-Aid for Scientific Research, type A (Grant No. 22246122) and type B (Grant No. 23360412) by Japan Society for the Promotion of Science.

¹M. Tabak *et al.*, *Phys. Plasmas* **1**, 1626 (1994).

²L. Willingale *et al.*, *Phys. Rev. Lett.* **106**, 105002 (2011).

³A. L. Lei *et al.*, *Phys. Rev. E* **76**, 066403 (2007); *Phys. Plasmas* **16**, 056307 (2009).

⁴S. Ivancic *et al.*, *Bull. Am. Phys. Soc.* **58**, 373 (2013), available online at <http://meetings.aps.org/Meeting/DPP13/Session/YO5.7>.

⁵T. J. Kessler, Y. Lin, J. J. Armstrong, and B. Velazquez, in *Laser Coherence Control: Technology and Applications*, edited by H. T. Powell and T. J. Kessler (SPIE, Bellingham, 1993), Vol. 1870, p. 95.

⁶P. B. Radha *et al.*, *Phys. Plasmas* **12**, 056307 (2005).

⁷A. J. Mackinnon, P. K. Patel, R. P. Town, M. J. Edwards, T. Phillips *et al.*, *Rev. Sci. Instrum.* **75**, 3531 (2004).

⁸S. L. Pape, P. Patel, S. Chen, R. Town, D. Hey, and A. Mackinnon, *High Energy Density Phys.* **6**, 365 (2010).

⁹R. P. J. Town *et al.*, *Bull. Am. Phys. Soc.* **50**, 123 (2005).

¹⁰D. S. Hey *et al.*, *Rev. Sci. Instrum.* **79**, 053501 (2008).